Broadband blueshift tunable metamaterials and dual-band switches

Nian-Hai Shen,[1] Maria Kafesaki,[1,2] Thomas Koschny,[1,3] Lei Zhang,[3] Eleftherios N. Economou,[1,4] and Costas M. Soukoulis[1,2,3,*]

[1]*Foundation for Research and Technology, Hellas (FORTH), Institute of Electronic Structure and Laser (IESL), P.O. Box 1527, 71110 Heraklion, Crete, Greece*
[2]*Department of Materials Science and Technology, University of Crete, 71003 Heraklion, Crete, Greece*
[3]*Department of Physics and Astronomy and Ames Laboratory, Iowa State University, Ames, Iowa 50011, USA*
[4]*Department of Computational and Data Sciences, George Mason University, Fairfax, Virginia 22030, USA*
(Received 27 February 2009; published 28 April 2009)

We propose a design and numerical study of an optically tunable metamaterial based on an electric-field-coupled inductor-capacitor resonator variant in the terahertz regime. In contrast to earlier proposed structures, we demonstrate that a blueshift of the resonance frequency under illumination can be accomplished with realistic material parameters and a broadband tuning range on the order of 40% has been demonstrated, which is found to be based on a photoconductivity-induced mode-switching effect. We also present a variant of this structure, which simultaneously possesses two resonance frequencies and can be used as an optically switchable dual-band resonator. Our all-optical modulators and switches may offer a step forward in filling the "THz gap."

PACS number(s): 78.20.Ci, 33.55.+b, 46.40.Ff, 42.25.−p

Due to exotic properties not attainable by naturally occurring materials, electromagnetic (EM) metamaterials, i.e., artificially engineered subwavelength composites, have led to a rapidly growing research field in recent years and resulted in many intriguing phenomena such as negative refraction,[1,2] diffraction-limit breaking imaging,[3–6] and cloaking.[7–9] Since the first experimental demonstration of negative refractive index metamaterials in the microwave regime,[1] research in fabrication, design, and application of metamaterials has been extended to a fairly wide range of the EM spectrum including far-, mid-, and near-infrared regimes and even optical frequencies.[10–12] Recently, semiconductors have been judiciously incorporated into metamaterial designs, aiming at lowering the intrinsic losses[13] or realizing dynamical control over the effective response[14–16] of the metamaterial. In particular, the development of dynamically controllable or tunable metamaterials in the infrared regime[14–16] enables the fabrication of new active terahertz (THz) devices such as notch filters and switches, opening a bright perspective in filling the THz gap.

Recent progress in metamaterial design has led to the realization of frequency-agile functionality, or tunability, in metamaterials.[16] Tunable metamaterials are designed to work at a variable frequency controlled by some external stimulus within a frequency band instead of operating at a fixed frequency only determined by their geometry. The resonant element in these metamaterials is an effective inductor-capacitor (LC) resonator, the resonance frequency ω_0 of which is strongly dependent on the effective capacitance C and inductance L, i.e., $\omega_0 \propto (LC)^{-1/2}$. In order to achieve agility of the working frequency, external stimulus-dependent tunable elements are necessary to be incorporated into the designs for altering L and/or C. Incorporating a photoconductive semiconductor material in the capacitive element in the LC resonator, C can easily be increased with illumination, which leads to a redshift tunability (working frequency decreases with increasing illumination power) as reported in Ref. 16. On the other hand, L is considerably harder to be

changed effectively. The reason for that is the finite saturation photoconductivity of the semiconductor which is much smaller than the conductivity of the metals. In regions of charge accumulation (as in the capacitor) this is less critical, but if significant current is flowing through the photoconductor (as in the inductor) the increased losses easily kill the resonance. Thus, the two hypothetical metamaterial designs for blueshift tunability (working frequency increases with illumination) proposed by Chen *et al.*[16] are difficult to implement. Consequently, alternative designs are highly desirable to realize blueshift tunable metamaterials using optically controlled photoconducting elements.

In this Rapid Communication, we present a design for blueshift tunability with a photoconductive semiconductor incorporated into the metamaterial. Our approach takes advantage of a novel variant of the electric-field-coupled LC (ELC) resonator.[17] It will be shown that the tuning can be implemented within quite a broad frequency range of as much as ~40% in the THz regime, and this is achieved through an effect of photoconductivity-induced mode switching. We also present a variation of this resonator which shows two strong resonances simultaneously, and a metamaterial device based on it can be utilized as a good dual-band switch. Our designs may offer greater flexibility for the applications of frequency-agile metamaterials and possess potential applications as tunable notch filters and multiband switches especially in THz regime.

Our basic ELC resonator design and the corresponding metamaterial are shown in Fig. 1. The ELC resonator is created by combining a rectangular-shape variant of a conventional two-gap ELC resonator (e.g., structure E1 in Ref. 18; see the dotted frame in Fig. 1) with its mirror image. By inserting photoconductive silicon within the two side gaps but not the central gap of the combined ELC resonator, we obtain the unit cell of the metamaterial. No magnetoelectric coupling exists for this geometry, and consequently bianisotropy is avoided due to the symmetry of the structure.[19] The metamaterial consists of a planar array of ELC resonators set
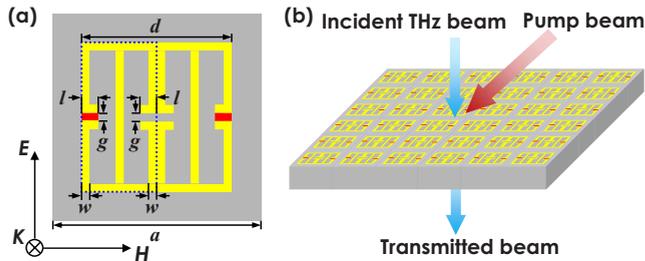
FIG. 1. (Color online) Schematic illustration of our designed metamaterial structure for broadband blueshift tunability. (a) Unit cell geometry viewed along the direction of propagation: Yellow part (bright in print), gray part, and red part (dark in print) are metal (gold), substrate (sapphire), and photosensitive semiconductor (silicon), respectively. $a=50$ μm, $d=36$ μm, $w=g=2$ μm, and $l=4$ μm. Both the gold and silicon are of 200 nm thick. Inside the dotted frame is the half-structure of our metamaterial design. The polarization of the normally incident THz wave is also indicated. **E**, **H**, and **k** represent electric field, magnetic field, and wave vector, respectively. (b) Perspective view of an array structure of our metamaterial design for testing.

up on the surface of a thick sapphire substrate.

We characterize our metamaterial by simulating the transmission through the sample, t_{MM}, normalized by that through a bare substrate (as reference), t_{sub}, i.e., $t(\omega)=t_{MM}/t_{sub}$.[14–16] All numerical simulations are performed using the commercial software CST Microwave Studio. A single unit cell as shown in Fig. 1(a) is adopted for the simulations with appropriate boundary conditions resembling actual conditions in a THz time-domain spectroscopy (THz-TDS) experiment. Almost all material parameters are chosen identical to those in Ref. 16. A lossy-metal model is utilized for gold (metallic parts of the resonator), the conductivity of which is $\sigma_{gold}=7\times10^6$ S/m. The photoconductive silicon is simulated with $\varepsilon_{Si}=11.7$ and a pump-power-dependent conductivity σ_{Si}. The sapphire substrate is taken as lossless dielectric with $\varepsilon_{sapphire}=10.5$. Notice that σ_{Si} is taken to be 1 S/m without illumination; to be realistic, we assume the upper limit under illumination of 50 000 S/m, which is the same as used for fitting the experimental results in Ref. 16.

Figure 2 shows the simulated normalized transmission spectra $t(\omega)$ for different silicon conductivities. At first,
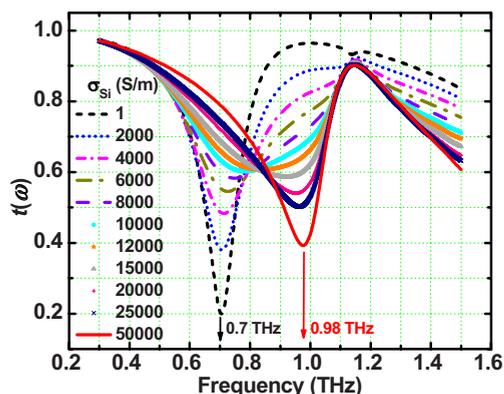

FIG. 2. (Color online) Simulated transmission spectrum of the metamaterial for different values of silicon conductivity.
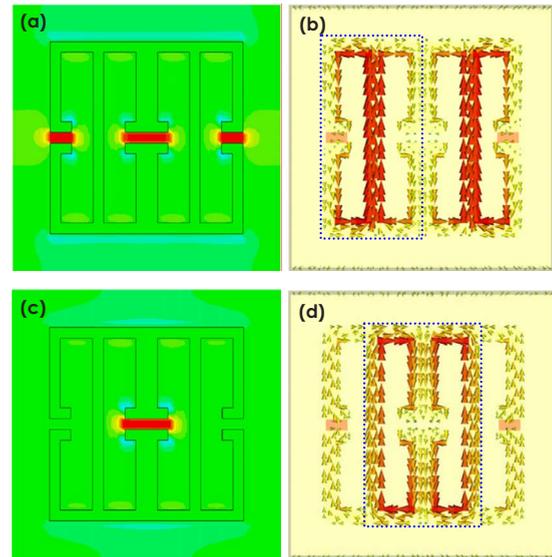

FIG. 3. (Color online) Distribution of electric fields and surface current densities at $\omega_0=0.7$ THz for $\sigma_{Si}=1$ S/m (a) and (b) and $\omega_0=0.98$ THz for $\sigma_{Si}=50\,000$ S/m (c) and (d), respectively. Parts within dotted frame in (b) and (d) are for roughly estimating the respective resonance frequency of the two cases.

without illumination, a transmission minimum $t(\omega)=20\%$ occurs near the resonance at 0.7 THz. With increasing photoconductivity of silicon (2000~6000 S/m), the resonance initially weakens, its linewidth broadens, and it starts to shift to higher frequencies. As σ_{Si} further increases (8000~12 000 S/m), the resonance continues to weaken and saturates at $t(\omega)\sim60\%$, while the blueshift is relatively significant. For σ_{Si} beyond 12 000 S/m, the resonance keeps shifting to higher frequencies, and its strength recovers gradually. Finally, for $\sigma_{Si}=50\,000$ S/m, the resonance dip in transmission spectrum $t(\omega)=39\%$ is located at 0.98 THz. Therefore, a fairly broad blueshift, as much as 40%, has been achieved without requiring unrealistically high photoconductivity; hence, our design should be easy to implement.[16]

In order to understand the mechanism leading to such a broadband tuning effect of our proposed metamaterial design, an intuitive and straightforward way is to investigate the distributions of electric fields and surface current densities at the resonance frequencies. Figure 3 shows the field and current distribution for cases with no illumination ($\sigma_{Si}=1$ S/m) and with heavy photodoping ($\sigma_{Si}=50\,000$ S/m) at their respective resonance frequencies. Obviously, the resonances of the two cases belong to very different modes, so the blueshift of the resonance frequency can be considered to be due to a *photoconductivity-induced mode-switching effect*. For strong illumination [Figs. 3(c) and 3(d)], the outer gaps of the ELC resonator are conducting and do not provide appreciable capacitive response. The "only" resonant mode in this case is the regular one-gap ELC resonator [shown within the dotted frame in Fig. 3(d)] with charge accumulation across the capacitor in the center and opposite inductive ring currents along the inner metal bars, simultaneously modified by the shunt inductance provided by the outer conductive paths. The magnetic moments of those currents cancel, and we are left with a resonant electric

response as expected for an ELC resonator. This resonance occurs at a frequency (here $\omega_0 = 0.98$ THz), which could be roughly estimated by that of the regular one-gap ELC resonator (the effect of shunt inductance offered by outer conductive paths should also be taken into account). The case of low illumination, in which the outer gaps are nonconducting, is more complicated. The resonance mode has opposite circular resonant currents in the two outer loops of the resonator, and simultaneously, circular currents also exist in the inner loops, while with opposite direction to that in the outer loops at either side of the resonator. The magnetic moments cancel but the electric moments provided by all three gaps add constructively. The result is a strong electric resonant response. If we (formally) split our ELC into two adjacent classical two-gap ELC resonators [shown within the dotted frame in Fig. 3(b)], this mode would be of the symmetric hybrid electric excitation, and the resonance frequency (here $\omega_0 = 0.7$ THz) could be approximately given by that of the single classical two-gap ELC resonator, leading to a relatively lower resonance frequency due to a higher capacitance with respect to that of a regular one-gap ELC resonator.[18] In principle, the low illumination case would also possess a mode with opposite polarizations across the central and the two outer gaps with similar current distribution (and resonance frequency) as the strong illumination mode above. (The antisymmetric electric and symmetric magnetic hybrid modes cannot be excited in either case because of the mirror symmetry of the structure with respect to the medial axis in **E** direction.) However, for the chosen geometry, the total electric moment of this mode vanishes such that it cannot be excited by the incident wave. Consequently, we only see a single low-frequency electric resonance at low illumination. Our blueshift tunable metamaterial actually works by switching between two different resonant modes via photoexcitation.

Additionally, we would like to mention that we also have considered another configuration, much similar to that adopted in Ref. 16, in which the silicon layer (600 nm thick) is between the metal layer and sapphire substrate and only the silicon located within the two outer gaps and beneath the metallic pattern is kept. Similarly, a 40% broadband blueshift tunability can be achieved upon some optimization to the dimension of ELC resonator (results not shown here).

As discussed above, for the metamaterial in Fig. 1(a), the low illumination high-frequency mode decouples by design. If, instead, we make the central and outer gaps in our ELC resonator (pure metallic pattern) deliberately different (by choosing $a = 50$ μm, $d = 36$ μm, $w = g_1 = 2$ μm, and $l_1 = g_2 = 6$ μm), the cancellation of the electric moments is lifted. We place the ELC resonator on top of the substrate and observe two resonances, corresponding to transmission dips: $t(\omega_1) \sim 20\%$ at $\omega_1 = 0.70$ THz and $t(\omega_2) \sim 20\%$ at $\omega_2 = 1.38$ THz. Figure 4 shows field and current distributions for the two resonant modes of such a metamaterial structure. Obviously, both resonances are electric in nature. This is confirmed by the resonant shape of the retrieved effective permittivity[20,21] at both frequencies (not shown). Therefore, the ELC resonator corresponding to the results shown in Fig. 4 can indeed be understood as an effective dual-band resonator. It is intriguing that, different from common dual-
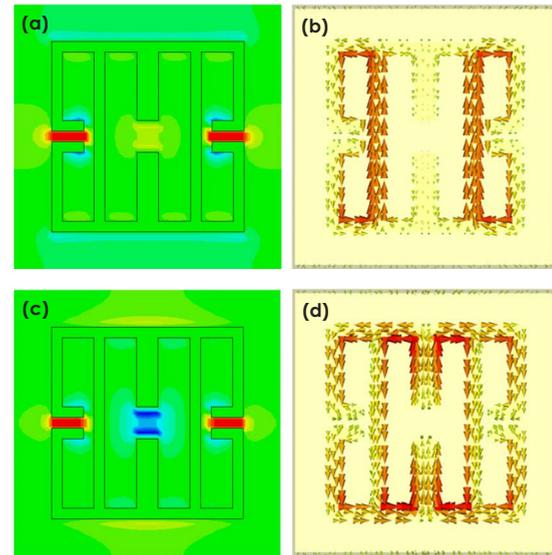

FIG. 4. (Color online) Distribution of electric fields and surface current densities at the two resonance frequencies of $\omega_1 = 0.70$ THz (a) and (b) and $\omega_2 = 1.38$ THz (c) and (d), respectively, for a metamaterial in which ELC resonator whose the central capacitance is much smaller than the outer ones is put on top of the substrate (no photosensitive silicon is incorporated).

resonant metamaterials which are based on two independent resonators of different size,[22] our design gives two resonances from a single structure. Very recently, a similar single-particle resonator integrating two resonant modes was proposed by Yuan *et al.*;[23] our design, however, appears to provide better uniformity of the resonance strength for the two modes. Due to the dual-resonant property of the ELC resonator it is a good candidate to build a dual-band switching metamaterial. The inset of Fig. 5 presents a possible configuration where a 600-nm-thick photoexcited silicon layer is used between the gold film (ELC resonator layer) and sapphire substrate. The simulated normalized transmission spectra for varying silicon conductivity are shown in Fig. 5. We
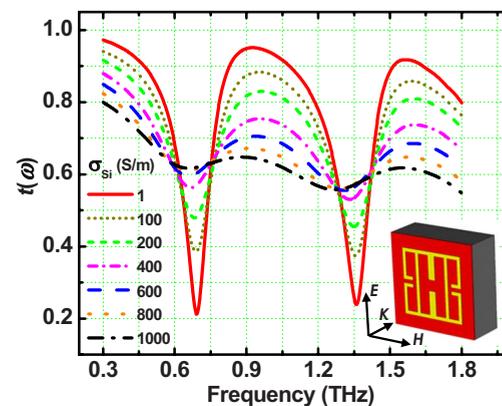

FIG. 5. (Color online) Simulated dual-band switching effect: transmission spectra as a function of silicon conductivity. The inset is the unit cell of the metamaterial for dual-band switch: A 600-nm-thick photosensitive silicon layer (red online and dark in print) is introduced between the metal film and substrate of the structure in Fig. 4(a).

find that with increasing photodoping in the silicon layer, the two sharp resonances that exist in the case with no illumination are simultaneously suppressed gradually with increasing illumination intensity by up to 40% and 35%, respectively, for rather small increase in photoconductivity. We noticed that the conductivity of metal layer plays an important role in determining the efficiency of the switching effect. We also simulated the same configuration with copper ($\sigma_{Cu} = 5.80 \times 10^7$ S/m) instead of gold, and photoconductive increases in $t(\omega)$ are 55% and 45%, respectively, at the two resonance frequencies (not shown).

In conclusion, we proposed a design for a blueshift tunable THz metamaterial based on an elaborate ELC resonator with embedded photoconductive material. In contrast to earlier proposed structures, we demonstrated that a ~40% blueshift of the resonance frequency under illumination can be achieved with realistic material parameters and illumination power densities. Our design offers greater flexibility in applications of frequency-agile devices. A variant of this structure can be used as an optically switchable dual-band resonator, simultaneously possessing two input frequencies.

---

*soukoulis@ameslab.gov

[1] R. A. Shelby, D. R. Smith, and S. Schultz, Science **292**, 77 (2001).

[2] J. B. Pendry, A. J. Holden, D. J. Robbins, and W. J. Stewart, IEEE Trans. Microwave Theory Tech. **47**, 2075 (1999).

[3] J. B. Pendry, Phys. Rev. Lett. **85**, 3966 (2000).

[4] Z. Jacob, L. V. Alekseyev, and E. Narimanov, Opt. Express **14**, 8247 (2006).

[5] Z. Liu, H. Lee, Y. Xiong, C. Sun, and X. Zhang, Science **315**, 1686 (2007).

[6] I. I. Smolyaninov, Y.-J. Hung, and C. C. Davis, Science **315**, 1699 (2007).

[7] J. B. Pendry, D. Schurig, and D. R. Smith, Science **312**, 1780 (2006).

[8] D. Schurig, J. J. Mock, B. J. Justice, S. A. Cummer, J. B. Pendry, A. F. Starr, and D. R. Smith, Science **314**, 977 (2006).

[9] W. Cai, U. K. Chettiar, A. V. Kildishev, and V. M. Shalaev, Nat. Photonics **1**, 224 (2007).

[10] C. M. Soukoulis, S. Linden, and M. Wegener, Science **315**, 47 (2007), and references therein.

[11] N. Liu, H. Guo, L. Fu, S. Kaiser, H. Schweizer, and H. Giessen, Nature Mater. **7**, 31 (2008).

[12] J. Valentine, S. Zhang, T. Zentgraf, E. Ulin-Avila, D. A. Genov, G. Bartal, and X. Zhang, Nature (London) **455**, 376 (2008).

[13] A. J. Hoffman, L. Alekseyev, S. S. Howard, K. J. Franz, D. Wasserman, V. A. Podolskiy, E. E. Narimanov, D. L. Sivco, and C. Gmachl, Nature Mater. **6**, 946 (2007).

[14] W. J. Padilla, A. J. Taylor, C. Highstrete, M. Lee, and R. D. Averitt, Phys. Rev. Lett. **96**, 107401 (2006).

[15] H.-T. Chen, W. J. Padilla, J. M. O. Zide, A. C. Gossard, A. J. Taylor, and R. D. Averitt, Nature (London) **444**, 597 (2006).

[16] H.-T. Chen, J. F. O'Hara, A. K. Azad, A. J. Taylor, R. D. Averitt, D. B. Shrekenhamer, and W. J. Padilla, Nat. Photonics **2**, 295 (2008).

[17] D. Schurig, J. J. Mock, and D. R. Smith, Appl. Phys. Lett. **88**, 041109 (2006).

[18] W. J. Padilla, M. T. Aronsson, C. Highstrete, M. Lee, A. J. Taylor, and R. D. Averitt, Phys. Rev. B **75**, 041102(R) (2007).

[19] W. J. Padilla, Opt. Express **15**, 1639 (2007).

[20] D. R. Smith, S. Schultz, P. Markos, and C. M. Soukoulis, Phys. Rev. B **65**, 195104 (2002).

[21] X. Chen, T. M. Grzegorczyk, B. I. Wu, J. Pacheco, and J. A. Kong, Phys. Rev. E **70**, 016608 (2004).

[22] Y. Yuan, C. Bingham, T. Tyler, S. Palit, T. H. Hand, W. J. Padilla, D. R. Smith, N. M. Jokerst, and S. A. Cummer, Opt. Express **16**, 9746 (2008).

[23] Y. Yuan, C. Bingham, T. Tyler, S. Palit, T. H. Hand, W. J. Padilla, N. M. Jokerst, and S. A. Cummer, Appl. Phys. Lett. **93**, 191110 (2008).